

# **Influence of the reinforcement in the compaction of the soil layers – an experimental analyses**

Oliveira, J. P.; Vidal, D. M.

*This document is an article written by Jessica Pereira Oliveira after her Master's thesis approval at Instituto Tecnológico de Aeronáutica/Brazil in 2018, supervised by Delma de Mattos Vidal. All written information you can find in her Portuguese thesis accessing: <http://www.bditabr.itabrag.com.br/> with the name: “Influência de reforço com geogrelha na qualidade de camadas de solo compactadas”*

## **Abstract**

Geosynthetic reinforcements are used for pavement structures and shallow fills as alternatives in the execution of roads over weak subgrades. The use of reinforcements involves a number of benefits, such as a better distribution of the traffic load and a higher lifetime of the pavement. Many researchers aim to analyze the reinforcement behavior and its characteristics under the cyclical loading of the trafficking during the lifetime of the paved roads, but little attention has been given to the quality of the compacted layer. This research discusses the influence of geogrid reinforcement during the compaction of reinforced soil layers, considering the ability to increase the resistance of the layer. As means for the work, a laboratory experiment was set simulating sections of the pavement with and without the insertion of a geogrid. Stiffness parameters were verified after the Plate Load test (PLT) and compared among them. The reinforcement enabled a high increase in the magnitude of the deformability modulus ( $E_{v2}$ ), even though the boundary conditions were limited.

**Keywords:** Compaction of soil, geogrids, reinforcement.

## **1. Introduction**

Soil compaction is an important technique used to promote soil conditions suitable for use in civil engineering constructions such as embankments, foundations and pavements. It is well known that the compaction process leads granular soils to exhibit better construction properties, such as increased stiffness and shear strength, and reduced permeability of the soil layer. In particular, for road structures, the strength properties are important parameters to evaluate in soil compacted layers taking into account the dynamic design loads to avoid shear failures or excessive settlements, according to project requirements.

Jéssica Pereira Oliveira, Programa de Pós-graduação em Infraestrutura Aeronáutica do Instituto Tecnológico de Aeronáutica, Brazil. e-mail: [jehpoliveira@gmail.com](mailto:jehpoliveira@gmail.com)  
Delma de Mattos Vidal. PhD. Programa de Pós-graduação em Infraestrutura Aeronáutica do Instituto Tecnológico de Aeronáutica, Brazil. e-mail: [delma@ita.br](mailto:delma@ita.br)

32 Frequently, in road designs, due to the high load volume and minimum deformation  
33 requirements, compaction of granular soils can become a problem if the subgrade below  
34 exhibits low bearing capacity. One of the techniques that allows a better execution of the soil  
35 layer compacted above weak subgrades is the insertion of geogrids as reinforcement (Berg et  
36 al., 2000).

37 Since the 1970s, geosynthetics, especially geogrids, have been used as base-  
38 reinforcement to afford better conditions for the execution of soil layers above weak subgrade,  
39 providing a rigid platform for road construction and increasing the subgrade bearing capacity.  
40 Moreover, several researches have shown that geogrids can improve the performance of  
41 pavement sections by reducing of the permanent deformation caused by vehicular loads. One  
42 of the main mechanics of geogrids in reinforcement function for roads is the lateral restraint  
43 (Abu-Farsakh, M., et al., 2016; Al-Qadi et al., 1994; Perkins et al., 2005; Perkins, 1999).

44 The lateral restraint, or confinement, is the effect due to the frictional and interlocking  
45 characteristics at the interface between the geosynthetic and the aggregate. The interaction  
46 between the aggregate and the geosynthetic allows the transfer of the shear load from the base  
47 layer to the geosynthetic reinforcements, thus reducing the shear stress developed in the upper  
48 layer. In addition, the shear resistance effect at the interface of the soil-reinforcement system  
49 increases lateral confinement and restraint the lateral movement of the layer above the  
50 reinforcement, and this increase in the confinement tension provides an increase in the layer's  
51 stiffness. Furthermore, this mechanism also provides better vertical distribution of tension in  
52 the subgrade due to the increase in the base elastic modulus and reduce shear stress along the  
53 top of the subgrade (Perkins, 1999; Berg et al., 2000; Zornberg & Gupta, 2010).

54 To obtain better results from this reinforcement mechanism a good soil-reinforcement  
55 interaction is needed, and that some characteristics of the reinforcement can enhance the lateral  
56 restraint, such as the geogrid apertures. This restraint between the soil and the reinforcement  
57 can provide a constructive platform capable of increasing the stiffness property of the layer  
58 above that reinforcement, even when in weak subgrades. Aware of this effect, if the stiffness of  
59 the layer above the reinforcement is increased, it can be expected that the compaction of this  
60 layer will be more efficient. However, the improvement of compaction due to reinforcement is  
61 little explored in the literature as a parameter for sizing or as a decision criterion in engineering  
62 projects. This can be attributed to the limited number of studies that address this topic and the  
63 difficulty of measuring this benefit (Perkins, 1999; Kwon & Tutumluer, 2009; Pei & Yang,  
64 2018).

65           This paper presents an experimental analysis to investigate the influence in the support  
66 capacity of the compacted layer due to the presence of geogrid reinforcement. The analyses  
67 were made comparing the traditional compaction parameters, as dry density and moisture  
68 content, and stiffness parameters of the layers of three section configurations (one without  
69 reinforcement and two reinforced sections). To verify the stiffness parameters, plate tests were  
70 performed to check the deformability modulus ( $E_{v2}$ ). Deformability modulus or reload modulus  
71 is an indicator of the bearing capacity of the soil or the flexible pavement under certain  
72 conditions simulated by loading and unloading a load plate. The load plate test is performed  
73 using fixed loading and unloading time steps and measuring settlement values.

## 74 **2. Compaction and reinforcement of the soil layers**

75 Soil compaction is one of the oldest and most commonly technique used to provide to the soil  
76 the stiffness properties that characterize the construction projects to which they are aimed. With  
77 the pioneering collaboration of Proctor, the process of soil densification by means of energy  
78 delivery under certain moisture content conditions is being researched showing itself as a very  
79 meaningful tool in soil construction projects.

80           Soil compaction process is based on obtaining a material with characteristics suitable  
81 for the intended application, and ensuring adequate conditions for construction during its  
82 service lifetime. The main benefits acquired in the soil compaction process are: increased soil  
83 strength and bearing capacity, in addition to reducing compressibility and permeability  
84 (Kodikara et al., 2018).

85           The soil compaction technique is characterized by the performance of a mechanical load  
86 in a specific condition of moisture for each type of soil, which will provide a dry specific weight,  
87 capable of guaranteeing the cited benefits during its service life. Achieving the uniformity of  
88 the compacted layer is decisive to successful compaction process. Many studies have shown  
89 that the primary reason for road failures are due to an uneven degree of compaction with gives  
90 insufficient bearing capacity for the soil layer. Commonly, in-situ spot tests are required for the  
91 quality control and uniformity of the layer. However, this conventional density control method  
92 has many issues associated, as sometimes weak compaction areas may be not identified and the  
93 measured density of top bound layer is limited to indicate the structural capacity of the entire  
94 pavement layers (Kodikara et al., 2018; Heitor et al., 2012; Chang et al., 2011).

95           In view of this procedure of relevant importance, numerous techniques and equipment  
96 have been developed to ensure the effective application of the load on the soil and the adequate  
97 uniformity of the layer. In addition, several techniques for controlling field compaction

98 parameters, such as nuclear density and strength modulus analysis, were developed and applied  
99 in addition to traditional moisture content and unit dry weight checks. Currently, Intelligent  
100 Compaction Technology is an effectively method able to record the soil response (i.e. soil  
101 stiffness or modulus) while the soil is being compacted (Heitor et al., 2012; Chang et al., 2011).

102 Furthermore, several factors influences directly the result of the compaction, among  
103 them there are: the soil origin, moisture content, the compaction energy, compactor travel speed  
104 and tire inflation pressure, the transmission mode of the energy and the number of pass, the  
105 environment condition, the preparation conditions, stiffness of the subgrade, the layer thickness  
106 and the influence of the reinforcement characteristics. Each of these factors has its peculiarity  
107 in relation to the final parameters reached in the layer through of the compaction (Vidal, 1985,  
108 Canillas & Vilas, 2001, Ferreira, 2008).

109 The stiffness of the constructive platform was approached by Arquie et al (1976) and  
110 Valeux and Morel (1980) as characteristic that directly influences the efficiency of the  
111 compaction process due to it provides greater homogenization of the layer density in depth. The  
112 energy applied during compaction should be related to the quality of the subgrade, since soil  
113 layers over subgrades with low stiffness under high energy loads are not able to absorb the load  
114 in depth in an equivalent manner, compromising deep soil compaction compromised. In this  
115 case, it is important to observe whether the applied energy is within the acceptable range with  
116 the bearing capacity of the subgrade or not.

117 Some author had observed that inserting a reinforcement material above a low bearing  
118 capacity soil the material compacted above the reinforcement presents increases in its strength  
119 properties. The stiffness of the reinforcement together with the confinement effect given by the  
120 interlocking of the grains and the aperture of the geogrid enable the applied energy to be better  
121 used. This phenomenon usually produces a better efficiency in the process of compaction  
122 (Kwon & Tutumluer, 2009; Pei & Yang, 2018).

123 Cancelli e Montanelli (1999) present in their research a high efficiency of the  
124 reinforcement in the execution of the layers, being verified an immediate improvement in the  
125 execution of section with small thickness above a weak subgrade with the presence of  
126 reinforcements. The absence of rut depth observed during the first 500 cycles of traffic over the  
127 reinforced layers in comparison with the rut depth of many millimeters on the layers without  
128 reinforcement allows the forecast a beneficial improvement of the reinforcement in the executed  
129 layer.

130 Klein et al. (2002) and Turano et al. (2000) demonstrated, using laboratory experiments  
131 in which boulder subbases were simulated over a low bearing capacity subgrade, with and

132 without reinforcement, that the presence of reinforcement can increase the bearing capacity of  
133 the reinforced layer by about 30 % in relation to the non-reinforced layer. The authors attribute  
134 this resistance improvement to the conditions of the interface soil-reinforcement, together with  
135 the confinement provided by the geogrid actuation mechanism.

136 Kwon and Tutumluer (2009) demonstrated from numerical modeling and field studies  
137 of geogrid base reinforce pavement systems, a stiffening effect around geogrid reinforcement  
138 and its result in improving the response and performance of the pavement. The stiffened zone  
139 observed around the geogrid reinforcement is mainly caused by the interlocking of aggregate  
140 particles in the geogrid apertures. The height of the influenced zone, where the load-induced  
141 permanent residual stresses locked in around the geogrid, was approximately 15 cm above and  
142 below the geogrid. An increase in horizontal confinement caused by residual stresses resulted  
143 in significant increases in the moduli of the base and subgrade layers in the proximity of the  
144 geogrid reinforcement.

145 Pei and Yang (2018) used a discrete element method (DEM) model to simulate the  
146 development of compaction-induced stress in a granular base course, with and without  
147 reinforcement. In this research was observed that geogrid reinforcement helps granular base  
148 courses to lock in additional compaction-induced stress during the roller compaction. This  
149 behavior is attribute to confining effect from the residual tensile stress in the geogrid, which  
150 increase with the number of compaction passes. Moreover, to mobilize the benefit of the  
151 geogrid reinforcement when the subgrade has low bearing capacity are needed more  
152 compaction passes.

### 153 **3. Materials and Methods**

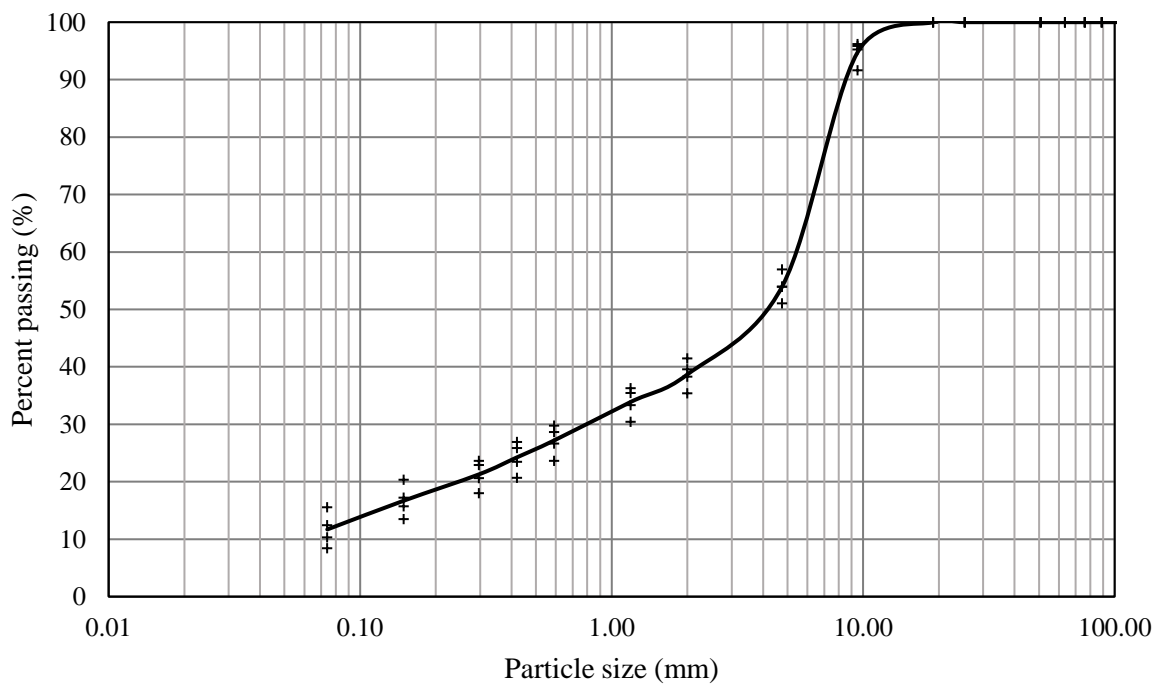
#### 154 3.1. Tests conception and materials

155 Aiming to gather experimental data to analyze the influence of the geosynthetic reinforcement  
156 in the improvement of the compaction of soils, laboratory tests were performed considering the  
157 superposition of the subgrade layer and the subbase layers with and without reinforcement  
158 elements, and with a separation element between them. In total, three tests were concluded with  
159 the following order: a test without the reinforcement element (referred to as E-1-SR) and two  
160 test with the reinforcement element. Between the reinforced tests, there was a variation in the  
161 stiffness of the reinforcement, where the first reinforcement has a low stiffness and the second  
162 has a high stiffness (referred to as E-2-GR1 and E-3-GR2, respectively).

163 The subgrade was composed by a mixture of two industrial clays prepared in the  
164 laboratory. The clays, classified as kaolinite and bentonite, had more than 99 % of passing

165 material through the sieve # 325 and they were mixed with the ratio 4:1. For the mixture there  
166 was a liquid limit of 74 % and plastic limit of 24 %, that is, a plasticity index of 50 %. In the  
167 execution of the test the water content used was of 32 %.

168 The subbase was simulated by a graded gravel, as can be seen in Figure 1. From the  
169 characterization tests, the material was classified by the HRB (Highway Research Board) and  
170 by the USCS (Unified Soil Classification System) standards as A-1-a and GW, respectively.  
171 The Modified Proctor test provided an apparent dry unit weight of 23.4 kN/m<sup>3</sup> and optimal  
172 moisture content of 6.1%. These parameters guided the preparation of the material through the  
173 experiment.



174

175 Figure 1: Particle size distribution curve for subbase material

176 Two biaxial geogrids with protective polymer coating (Huesker Basetrac® Grid PET 40 and  
177 Huesker Duo 80/80B 25FT, referred to as GR1 and GR2, respectively) were used in the test  
178 sections. These products were chosen to provide a range of parameters thought to control  
179 reinforcement ability in the compaction of soil layer. Moreover, these geogrids have been  
180 recommended for base reinforcements, and the choice for them was based on related research  
181 which used the similar aperture for a similar particle-size distribution of the subbase material.  
182 The physical and mechanical properties of these geosynthetics as provided by the manufacture  
183 are presented in Table 1.

184

Table 1 Geosynthetic material properties (from the manufacturer)

Properties	Unit	Test standard	Geogrid GR1	Geogrid GR2
Aperture Size (MD x CMD)	mm	-	25 x 25	30 x 30
Mass per unit area	g/m <sup>2</sup>	EN ISO 9864	257	714
Tensile Strength (MD)	kN/m	EN ISO 10319	48,9 ± 0.3	92,4 ± 0.5
Tensile Strength (CMD)	kN/m	EN ISO 10319	44,2 ± 0.4	90,6 ± 1.2
Strain at maximal Tensile Strength (MD)	%	EN ISO 10319	10,2 ± 0.2	9,2 ± 0.5
Strain at maximal Tensile Strength (CMD)	%	EN ISO 10319	9,9 ± 0.2	7,9 ± 0.3
Stiffness at 2 % strain (MD)	kN/m	EN ISO 10319	580	970
Stiffness at 2 % strain (CMD)	kN/m	EN ISO 10319	530	1055

MD - machine direction    CMD - cross machine direction

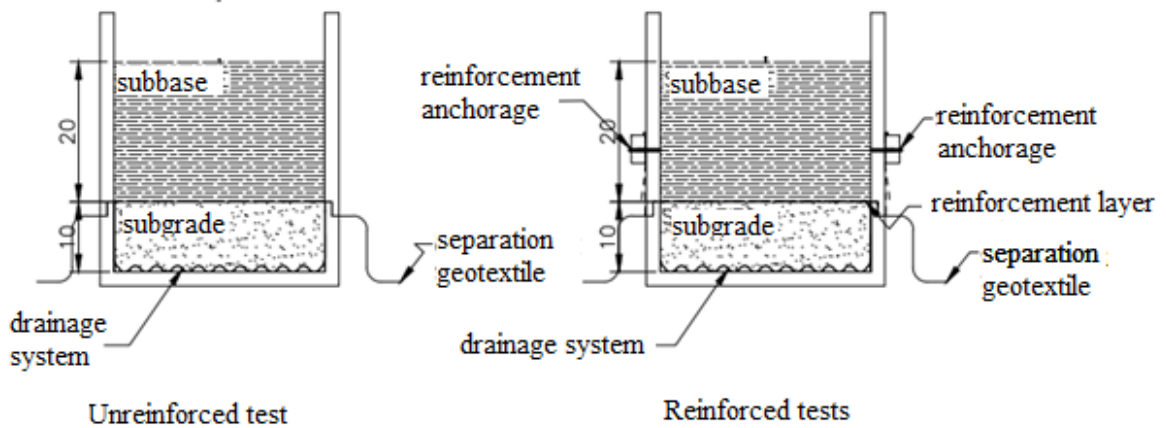
186            A non-woven geotextile with high deformability was used with separation and filtration  
 187 functions between the subgrade and subbase layers to guarantee there was no mixture of the  
 188 adjacent materials.

189            In execution of the tests each compacted layer had its physical (density and water  
 190 content) and mechanical characteristics evaluated. The mechanical behavior was evaluated  
 191 through plate loading tests, following the instructions of the German standard DIN 18134:2012,  
 192 which provided the deformability modulus ( $E_{v1}$  e  $E_{v2}$ ) of each layer.

193            These compaction tests were performed in a wood box, constructed with two  
 194 compartments, an inferior compartment for the subgrade and a superior compartment for the  
 195 subbase. This configuration was required so there would be an anchorage of the geogrid on the  
 196 outside of the box. The box had internal lateral dimensions of 30 cm x 30 cm and height of 40  
 197 cm. The overall nominal design cross-section of the tests sections is given in Figure 2.

198            To avoid lateral displacements through the box walls, a locking system made of steel  
 199 angles was placed on the outer sides of the box in both compartments. In addition, to reduce the  
 200 friction with walls and soil, was used employing on the inner side of the box two plastic sheets  
 201 with graphite grease between the sheets.

202            Moreover, a drainage system was installed under the subgrade with the goal to avoid  
 203 that an excess of water could influence the results. This system, made up of a geomembrane, a  
 204 geospacer, and a filter geotextile, allowed to verify the existence of water carried to the drainage  
 205 system during the test.



206

207

Figure 2: Test configuration (units in centimeter)

208

209

210

211

212

213

214

The applied force was visually monitored by a load cell placed directly over the receiving load surface. For the displacement measurements, two extensometers were installed in each step to observe the vertical displacement of the load plate tests in the subbases and for the verification of the stabilization of the settlements in compaction of the subgrade. The data acquisition of the extensometers was performed by connecting them to a computer, where an acquisition software collected the data from extensometers and recorded the average speed and the total displacement of the settlement for every 10 seconds of time.

215

### 3.2. Compaction process

216

217

218

219

The subgrade was compacted statically in three layers with  $60 \text{ kN/m}^2$  loads (light compactor) applied over all of its surfaces through a rigid plate until the settlement velocity was inferior to  $0.02 \text{ mm/min}$ . At the end of the execution of the subgrade, the deformability modulus was measured as explained in the Section 3.3.

220

221

222

223

The compaction of the subbase layer was subdivided into two layers. Each layer received static loads of  $150 \text{ kN/m}^2$  (Modified compactor) applied through a rigid plate over a third of the surface area ( $28 \text{ cm} \times 9,5 \text{ cm}$ ), during an interval of 10s, simulating the passing of a static roll.

224

225

226

227

228

The passing procedure was performed from the left to the right and after from the right to the left, repeating the process of loading and unloading four times in each layer, that is, simulating eight passing for each layer. At the end of the compaction of each layer, the height of the layer and its deformability moduli ( $E_{v1}$  and  $E_{v2}$ ) were measured as explained in the Section 3.3.

229

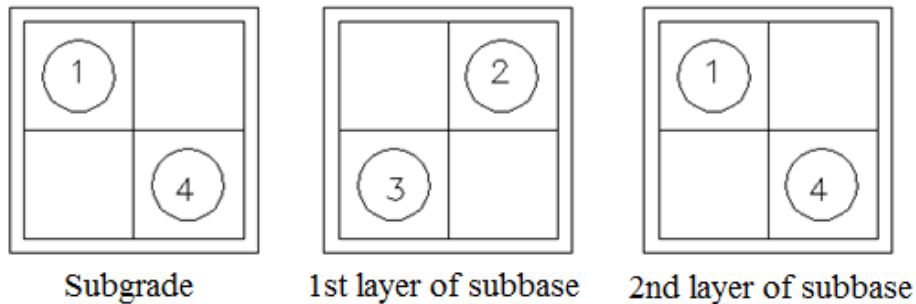
230

For began the experiment without reinforcement the first step of compaction was performed in loads of  $50 \text{ kN/m}^2$  for 10 s until to reach the  $150 \text{ kN/m}^2$ , just to calibrate the

231 apparatus. It was noted the necessity of adjustment of the high in load applicator due to the  
232 settlement observed. This adjustment of the high was necessary to all experiment, thus, in first  
233 three steps, the load of 150 kN/m<sup>2</sup> was applied, but the adjustment was also needed. The time  
234 of 10 s was considered only after the vertical displacements could occur without a new height  
235 adjustment in the loading system.

### 236 3.3. Finding the deformability modulus ( $E_{v1}$ e $E_{v2}$ ) of the compacted layers

237 For each compacted layer, it was planned a disposition of the tests to verify the deformability  
238 modulus ( $E_{v1}$  e  $E_{v2}$ ). The area of the box was divided into four quadrants. For each layer, the  
239 plate test was made in two diagonal quadrants as presented in Figure 3, exchanging the  
240 quadrants through the layers so the test in one layer would not interfere in the next test of the  
241 superior layer.



243 Figure 3: Plate load test quadrants for each layer

244 The plate test followed the procedure described by the German standard DIN  
245 18134:2012 with exception of the plate dimension. Considering the area of the box and the  
246 thickness of the layers, it was decided to use a plate with 100 mm of the diameter so the next  
247 layer would not influence in the results, especially so the reinforcement would not directly  
248 influence in the settlements measured. The distance from the plate to the box wall was  
249 approximately 40 mm and the influence of the boundary condition was not considered, as this  
250 procedure was performed in ever test boxes, and these experiments are only for comparison  
251 between them.

252 For the subgrade, the plate test was done with four stages of loading until to reach  
253 approximately twice of the compaction load. The sequence was of 20 %, 40 %, 70 % and 100  
254 % of the maximum loading. Then, it was done two stages of unloading following the withdrawal  
255 of 60 % and 40 % of the maximum load. According to DIN 18134:2012, the loading was kept  
256 unaltered until the settlement velocity would become lesser than 0.02 mm/min in each stage,  
257 then, it proceeded to the next step of the loading or unloading. For the subgrade layer, the

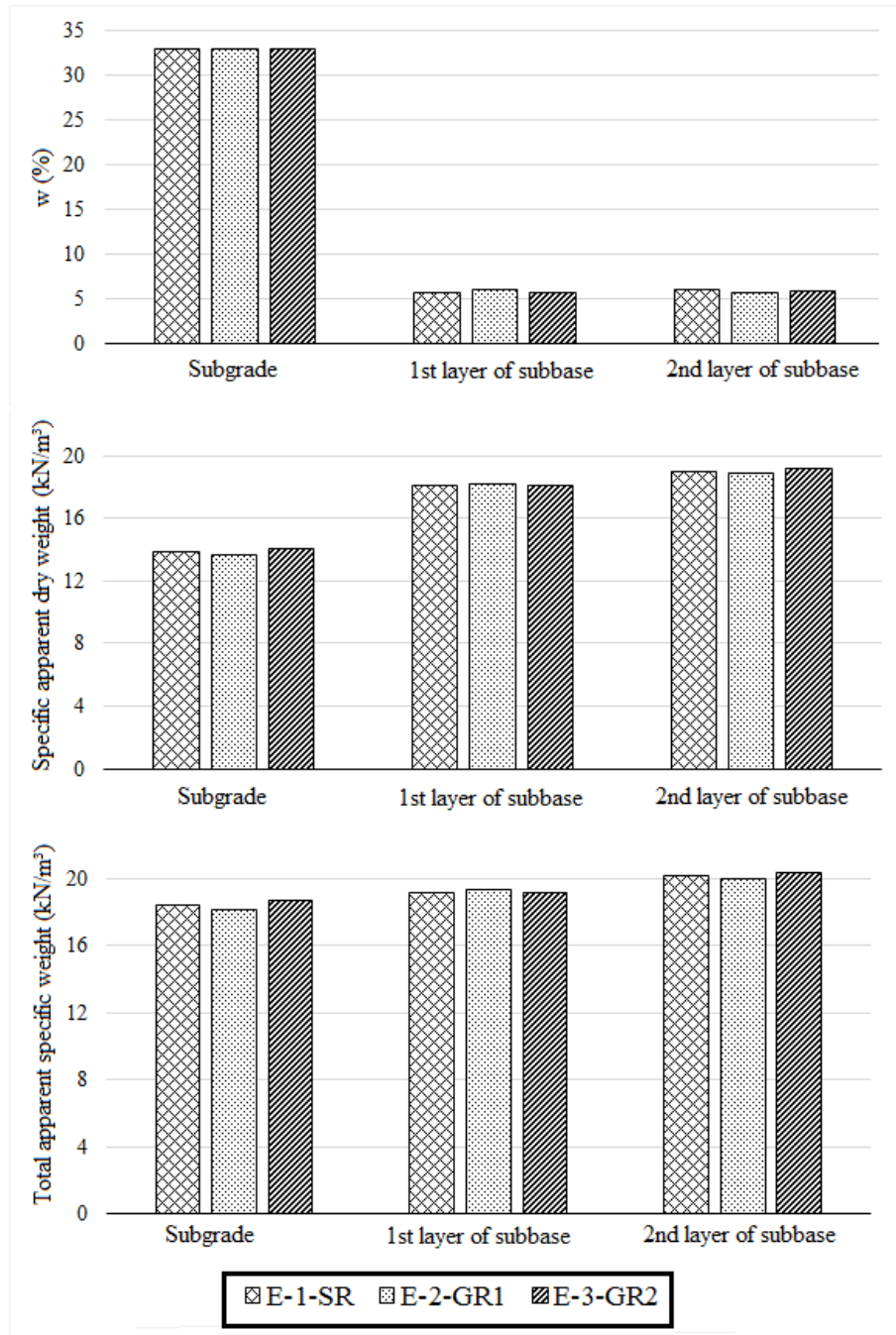
258 standard does not require the reloading, but in this experiment, in order to calculate the  $E_{v2}$  of  
259 the subgrade, the reloading was performed in at least one of the quadrants for each test.

260 For the subbase, it was performed 15 stages of loading, being 2 cycles of loading and 1  
261 cycle of unloading. The maximum loading provided was approximately twice of the  
262 compaction load applied. The first loading process was performed in 6 stages with similar  
263 increments up to the maximum load. The unloading was performed in 3 stages, in sequence of  
264 50 %, 25 % and 25% of the maximum load, then, followed by the second loading process in 5  
265 stages with similar increments, as it was in first loading. Each loading or unloading stage was  
266 maintained for a period of time of 1 minute, as recommended by DIN 18134:2012.

#### 267 **4. Results and discussion**

268 The results obtained by the compaction parameters such as water content and estimated dry and  
269 total apparent specific weight are presented in Figure 4. The values for the deformability  
270 modulus ( $E_{v1}$  e  $E_{v2}$ ) obtained in the plate loading tests for each quadrant are presents in Figure

271 5



272

273

Figure 4: Compaction parameters

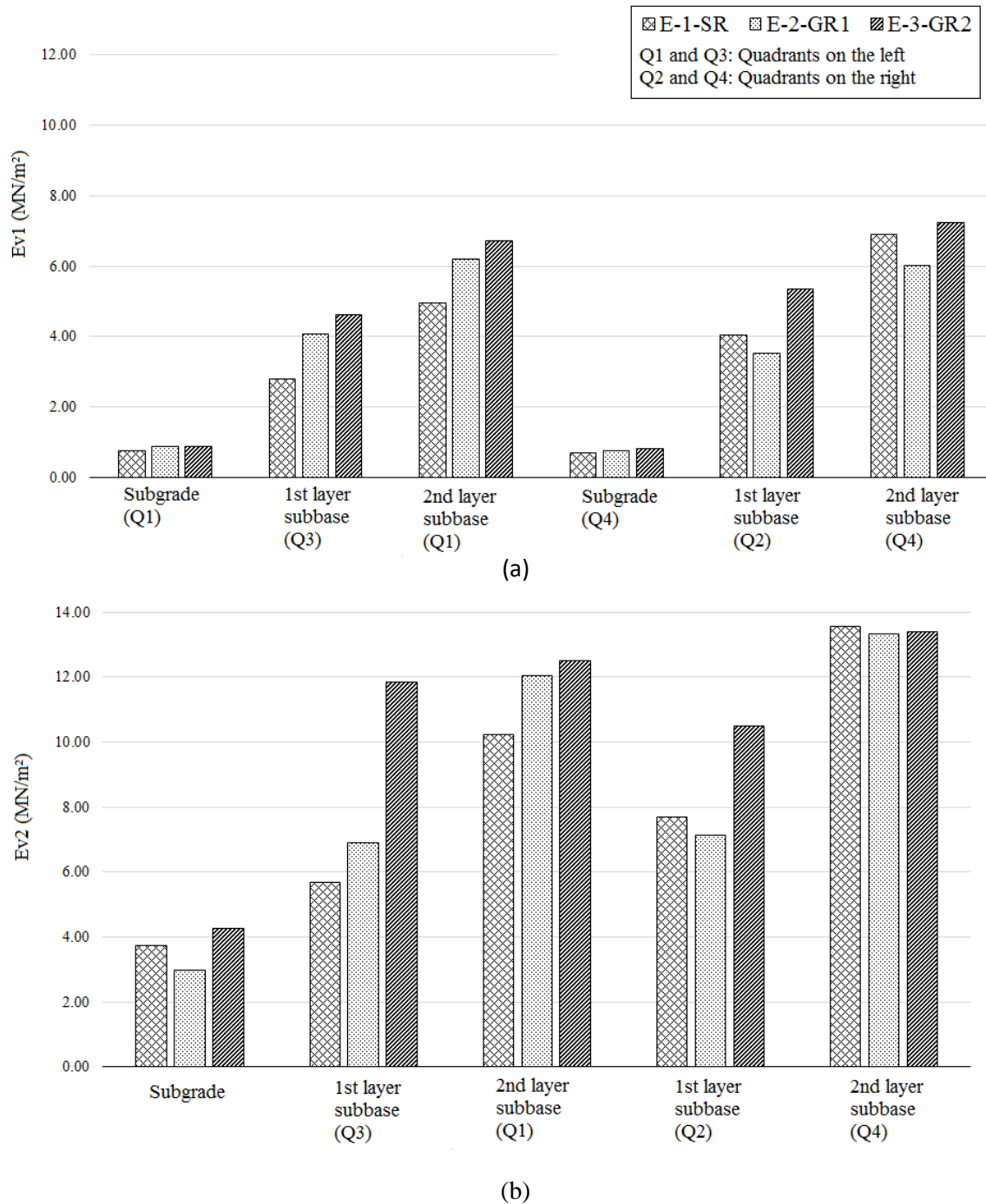


Figure 5: Deformability Modulus (a)  $E_{v1}$ , (b)  $E_{v2}$

274

275

276

277

278

279

280

281

As the experiments were disassembled, the capacity of the reinforcement to preserve the integrity of the bottom of the subbase was noted. By raising the upper box in the experiment without the reinforcement, the subbase soil disaggregated, as for in the cases with reinforcements the granular material of the base was kept confined by the geogrid, even when the aperture was much bigger than the size of the grains.

282 4.1. Compaction parameters analysis

283 From the results presented, it was noted that the mean density obtained were close to each other  
284 in all the tests. The density values for the subbase layer were little affected by the presence of  
285 the reinforcement. It stands out that the second layer of the subbase presented a density a little  
286 higher, as it was expected. From the values of the specific weight obtained for the subbase, it  
287 appears that the degree of compaction did not exceed 82 % of the Modified Proctor Test, even  
288 for the second layer.

289 During the execution of the compaction test, at the beginning of the compaction, with  
290 the loading plate on the left side of the box, the material on this side of the layer was moved to  
291 the right side during loading, providing this side with a higher final height in the layer. The  
292 lateral confinement of the box limited the movement of the material leading to a higher  
293 concentration of the material in the right part of the box.

294 4.2. Analysis of the deformability modulus

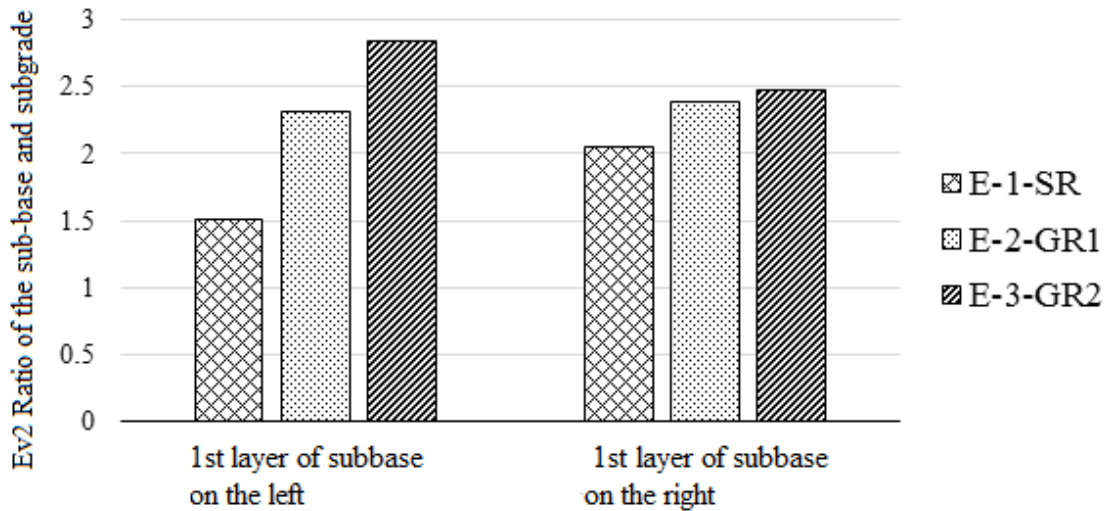
295 For a better understanding between the deformability modulus of the tests, it was prudent to  
296 separate the box on the left and right sides, given the influence of the compaction path process  
297 and the lateral confinement. This effect was observed especially during the first passing for all  
298 tests. In the case of the test E-1-SR, this ascending movement from the soil to the right side was  
299 more evident.

300 On the left side quadrants, where the compaction was done first, there was a significant  
301 improvement in Ev2 modulus due to the reinforcement. As of on the right side of the box, the  
302 reinforcement contributed less to the improvement of the deformability modulus of the first  
303 layer and nothing to the second layer, being this fact probably related to the aforementioned  
304 phenomenon of the lateral confinement during the compaction. As can be seen in (b)

305 Figure 5, it is noted that the first and second layers of the right side (quadrants Q2 and  
306 Q4) of the reinforced layers presents a deformability modulus smaller than what was observed  
307 for the layer without the reinforcement material. However, the quadrants located on the left side  
308 present more significant values of deformability modulus to compare the reinforced and non-  
309 reinforced section.

310 To evaluate the difference between the reloading modulus of the subgrade of the three  
311 tests, Figure 6 presents the relation between the modulus of the first layer of the subbase and  
312 the subgrade. There is a tendency of reinforcement to provide an increase proportional to the  
313 geogrid stiffness for both sides of the box, considering that the average stiffness at 2% of GR2  
314 (average of MD and CMD values) is 82% higher than the average of GR1. There is also an

315 increase in less intensity on the right side of the box, where, due to the conditions mentioned,  
 316 the E-1-SR test showed a high  $E_{v2}$  value.



317

318

Figure 6: Relation between  $E_{v2}$  of the first layer of the subbase and subgrade

319 Table 2 presents the percentage of the gains of the reinforced subbase layers in relation  
 320 with the non-reinforced layers, normalizing the  $E_{v2}$  modulus of the subbase layers in relation to  
 321 the modulus of the respective subgrade layer. To better understand the significance of these  
 322 values, is interesting to remember that the average stiffness at 2% of GR2 is 82% greater than  
 323 that of GR1.

324

Table 2 Reinforced subbase layer increase percentage

Geogrid	1st layer on the left	2nd layer on the left	1st layer on the right	2nd layer on the right
GR1	52	48	16	24
GR2	84	8	20	-13

325

326

327

328

329

330

331

332

333

Based solely on the values obtained by the quadrants on the left side, the insertion of the reinforcement provided, in both tests, a gain in the deformability modulus higher in the first layer than for the second layer. This behavior was expected since the inferior subbase layer already is a stiffer constructive platform for the second layer. As for the first layer, which was in direct contact with the subgrade, the stiffness gain at the interface provided by the reinforcement contributed to better compaction and a higher deformability modulus, proportional to the stiffness of the reinforcement. For the second layers, as mentioned, it was observed that the reinforcement did not significantly influence the stiffness gain, even showing no gain for the E-3-GR2 test.

334 **5. Conclusions**

335 The performance of the geogrid in the contribution of the properties of the soil-reinforcement  
336 system is subject of many researches and its benefits are evident. However, the efficiency of  
337 the reinforcement in the process of compaction is little discussed in the literature.

338 The test executed in this research enabled the conclusion that the reinforcement  
339 contributes to the improvement of the quality of the compacted layer above it, which can be an  
340 important characteristic for road constructions. The insertion of reinforcements provides a  
341 significant improvement for the deformability modulus of the first compacted layer above a  
342 subgrade with low bearing capacity and this gain is directly proportional to the stiffness of the  
343 reinforcement, as was observed by Kwon and Tutumluer (2009).

344 The values for the apparent specific weight of the layers compacted above a subgrade  
345 with low bearing capacity have no significant changes with the insertion of reinforcement in  
346 the cases tested. Probably the adoption of an identical compaction process for the reinforced  
347 and non-reinforced cases did not allow to achieve bigger densities that would be achievable for  
348 the reinforced case if the compaction energy was higher. Perhaps, with more compaction energy  
349 the increase in modulus increase would be more significant, as suggest Pei and Yang (2018).

350 The deformability modulus ( $E_{v2}$ ) of the subgrade layer has strict relation with the need  
351 for reinforcement. For the reinforcement to be considered necessary, the behavior of the lower  
352 layer after many repeatedly loadings should continue critical, that is, its stiffness should be little  
353 benefited by the application of compaction loads on the superior layers because these layers  
354 gains its stiffness during the compaction of the superior layer. The reinforcement may not be  
355 necessary, presenting low efficiency.

356 The relation between the grid aperture and the size of the grains presents a condition to  
357 be considered when proposing reinforced solutions to the section, given that besides the high  
358 stiffness of the reinforcement, this should also guarantee a better interlocking among the grains  
359 in a way to increase the efficiency over time (Das & Sivakugan, 2016). In this case the GR2,  
360 despite its aperture 7 times the  $d_{50}$ , showed the best interlocking, may be there is an ideal  
361 opening range for the interlock that goes beyond the value suggested by literature, however,  
362 future research should be explored to ascertain this issue.

363 To obtain a more expressive relation of the reinforcement in the compaction and to be  
364 able to separate the reinforcement influence during compaction and during cyclic loading, more  
365 studies are necessary, considering field and laboratory tests.

366 **References**

- 367 Arquie, G; Machet, Jm; Morel, G. (1976). Compactage des assises de chaussées – choix du  
368 matériel de compactage. BLLPC n.86, pp 113-124.
- 369 Al-Qadi Imad L., Brandon Thomas L., Valentine Richard J., Lacina Bruce A., Smith Timothy  
370 E. (1994) Laboratory evaluation of geosynthetic-reinforced pavement sections.  
371 *Transportation Research Record*, v. 1439, pp. 25-31.
- 372 Abu-Farsakh, M., et al., (2016). Performance of geosynthetic reinforced/stabilized paved  
373 roads built over soft soil under cyclic plate loads, *Geotextiles and Geomembranes*, n.44(6).
- 374 Berg, R. R.; Christopher, B. R.; Perkins, S. (2000) Geosynthetic Reinforcement of the  
375 Aggregate Base/sub-base Courses of Pavement Structures. Roseville, MN: AASHTO  
376 Committee 4e, 190 p.
- 377 Cancelli, A.; Montanelli, F. (1999). In Ground Test for Geosynthetic Reinforced Flexible  
378 Pavement Roads. *Proceedings Geosynthetics '99 Conference*, Boston, USA.
- 379 Canillas, Emmanuel & Salokhe, Vilas. (2001). Regression analysis of some factors  
380 influencing soil compaction. *Soil and Tillage Research*. 61. 167-178.
- 381 Chang, G.K., Xu, Q., Rutledge, J.G., Horan, B., Michael, L., White, D.D., & Vennapusa, P.K.  
382 (2011). Accelerated Implementation of Intelligent Compaction Technology for Embankment  
383 Subgrade Soils, Aggregate Base, and Asphalt Pavement Materials. *Federal Highway*  
384 *Administration*, report n° FHWA-IF-12-002.
- 385 Das, Braja M.;Sivakugan, Nagaratnam (2016). Fundamentals of Geotechnical Engineering. 5  
386 ed. Cengage Learning, p.755-756.
- 387 Ferreira, C. J. (2008). Avaliação estrutural de pavimento experimental reforçado com  
388 geogrelha. *Dissertação de Mestrado* – Instituto Tecnológico de Aeronáutica, São José dos  
389 Campos, São Paulo, 150 p.
- 390 Klein, R. J.; Vidal, D. M.; Rodrigues, R. M. (2003). Estudo dos efeitos nas propriedades do  
391 material compactado em obras de reforço de base de pavimentos com geossintéticos. *In: IV*  
392 *Simpósio Brasileiro de Geossintéticos*, Porto Alegre - RS: AMBS e IGS-Brasil;
- 393 Kodikara, Jayantha & Islam, Tanvirul & Sountharajah, Arooran. (2018). Review of Soil  
394 Compaction: History and Recent Developments. *Transportation Geotechnics*.
- 395 Kwon, J., & Tutumluer, E. (2009). Geogrid Base Reinforcement with Aggregate Interlock and  
396 Modeling of Associated Stiffness Enhancement in Mechanistic Pavement Analysis.  
397 *Transportation Research Record*, 2116(1), 85–95.

398 Pei, Te & Yang, Xiaoming. (2018). Compaction-induced stress in geosynthetic-reinforced  
399 granular base course – A discrete element model. *Journal of Rock Mechanics and*  
400 *Geotechnical Engineering*, p.669-677.

401 Perkins, S. W., Bowders, J. J., Christopher, B. R., & Berg, R. R. (2005). Geosynthetic  
402 reinforcement for pavement systems: US perspectives. *In International Perspectives on Soil*  
403 *Reinforcement Applications* (pp. 1-13).

404 Perkins, S.W. (1999). Mechanical Response of Geosynthetic-Reinforced Flexible Pavements,  
405 *Geosynthetics International*, v. 6, n. 5, pp. 347-382.

406 Turano Jr, J.; Vidal, D. M.; Rodrigues, R. M.. (2000) Increase of strenght and compaction  
407 efficacy by insertion of a geogrid in a granular base layer. *In: II European Geosynthetics*  
408 *Conference, Bologna*. v. 1. pp. 443-448.

409 Valeux, J.C.; Morel, G. (1980). Influence of bearing capacity of underlying materials on the  
410 compaction of pavement layers. *In: International Conference on Compaction, Editions*  
411 *Anciens ENPC, Paris*, v.2, pp. 475-480.

412 Vidal, D. (1985). Simulation Numérique non linéaire de la Construction de Remblais en  
413 Matériaux Isotrope et Anisotrope. *Thèse*. Université Scientifique et Médicale de Grenoble.  
414 France. 221 p.

415 Zornberg, Jorge.; Gupta, R. (2010). Geosynthetics in pavements: North American  
416 contributions. *In 9th International Conference on Geosynthetics, Brazil, 2010*